Neuropharmacology 63 (2012) 692–700

Contents lists available at SciVerse ScienceDirect

Neuropharmacology

journal homepage: www.elsevier.com/locate/neuropharm

Activation of ATP-sensitive potassium channels as an element of the neuroprotective effects of the Traditional Chinese Medicine MLC901 against oxygen glucose deprivation

H. Moha Ou Maati, M. Borsotto, F. Chatelain, C. Widmann, M. Lazdunski*, C. Heurteaux*

Institut de Pharmacologie Moléculaire et Cellulaire, Centre National de la Recherche Scientifique (CNRS, UMR6097), Université de Nice Sophia Antipolis, 660 Route des Lucioles, 06560 Valbonne, France

ARTICLE INFO

Article history:
Received 20 December 2011
Received in revised form
30 April 2012
Accepted 24 May 2012

Keywords:
K_{ATP} channel
MLC901
Ischemia
Hypoxia
Calcium imaging

ABSTRACT

NeuroAid (MLC601 and MLC901), a Traditional Medicine used in China for patients after stroke has been reported in preclinical models of ischemia to induce neuroprotection and neuroplasticity. This work shows the effects of MLC901 on an *in vitro* model of oxygen glucose deprivation (OGD). MLC901 prevents neuronal death induced by 120 min OGD and decreases the exaggerated Ca^{2+} entry in mature cortical neurons exposed to 120 min OGD. The neuroprotective effect of MLC901 is associated with a large hyperpolarization of ~20 mV which is antagonized by glibenclamide, the specific inhibitor of K_{ATP} channels. In addition MLC901 strengthens the activation of K_{ATP} channels. MLC901 has been directly shown to act as an activator of K_{ATP} channels as potent as the classical K_{ATP} channel opener. The capacity of MLC901 to produce a large hyperpolarization, particularly in neurons that have suffered from energy deprivation probably plays an important role in the neuroprotective effects of this traditional medicine that comes in addition to its previously demonstrated neuroregenerative properties.

1. Introduction

MLC601 (NeuroAid) shows promising results in post-stroke recovery of patients (Chen et al., 2009). It combines 9 herbal and 5 animal components. A simplified formula of MLC601 called MLC901 (NurAid II) based on its 9 herbal components is also now available (Heurteaux et al., 2010). MLC601 treatment is currently used in several countries both in Asia and in the Middle East for stroke patients. A multicenter, randomized, double-blind placebo-controlled study to investigate CHInese Medicine MLC601 Efficacy on Stroke recovery (CHIMES) is ongoing in Asia (Venketasubramanian et al., 2009). The safety of MLC601 on hemostasis, hematology and biochemistry has been established both in normal subjects and stroke patients (Gan et al., 2008; Young et al., 2010). Its apparent efficiency in improving cerebral blood flow velocity (Shahripour et al., 2011) and stroke rehabilitation, even several months after stroke (Chen et al., 2009) are strong arguments to pursue fundamental studies to better understand in animal models as well as at the cellular and molecular levels how MLC601 and MLC901 work. We have previously demonstrated with rodents that both MLC601 and MLC901 improve survival, protect the brain from a focal ischemic injury and drastically decrease functional deficits induced by stroke (Heurteaux et al., 2010). Moreover in a model of global ischemia, mimicking a cardiac arrest, MLC901 has been shown to prevent both necrosis and apoptosis of hippocampal neurons and to improve both motor and cognitive recovery (Quintard et al., 2011). Among the many possible mechanisms of the beneficial effects of MLC601 or MLC901 against ischemia we have established that they stimulate BDNF expression, enhance neurogenesis, promote cell proliferation and stimulate neurite outgrowth. Moreover the Akt pathway, which is known to be involved in cell survival appears to be critical in the MLC901 protective effect, and the Traditional Chinese Medicine (TCM) prevents the exaggerated lipid oxydation produced by ischemia (Quintard et al., 2011).

The brain requires continuous oxygen and glucose supply to maintain function. Neurons are extremely vulnerable to hypoxic injury. In clinical conditions such as cerebral ischemia permanent loss of neuronal functions occurs within minutes of severe hypoxia. Ionic homeostasis (Na^+, K^+, Ca^{2+}, Cl^-) of brain tissue is greatly disturbed and neurons depolarize following oxygen deprivation leading to swelling, calcium overload, and subsequently to the death of neurons (Dirnagl et al., 1999; Lee et al., 2000). Generally, neurons start changing their ion permeability and levels of intracellular ATP decline within seconds of hypoxia. Because under ischemic conditions the intracellular ATP level falls and substantially, because the ADP/ATP

* Corresponding authors. Tel.: +33 4 93 95 77 84; fax: +33 4 93 95 77 04.
E-mail addresses: lazdunski@ipmc.cnrs.fr (M. Lazdunski), heurteau@ipmc.cnrs.fr (C. Heurteaux).

0028-3908/$ – see front matter © 2012 Elsevier Ltd. All rights reserved.
doi:10.1016/j.neuropharm.2012.05.035

ratio is drastically increased, K_{ATP} channels are activated resulting in membrane hyperpolarization (Amoroso et al., 1990; Ashcroft and Ashcroft, 1990). This hyperpolarization prevents for a short period a massive release of excitotoxic glutamate. A sustained activation of K_{ATP} channels has been proposed as a possible way to be neuroprotective against brain ischemia and indeed K_{ATP} openers have been shown to be neuroprotective (Blondeau et al., 2000; Heurteaux et al., 1993, 1995; Lauritzen et al., 1997; Liss and Roeper, 2001).

The present study was designed to investigate the therapeutic effectiveness of MLC901 in a cellular model of oxygen glucose deprivation, which specifically mimics the rapid depletion of oxygen and glucose seen under ischemic conditions *in vivo*. It has demonstrated the beneficial effects of MLC901 on calcium influx and cell death. MLC901 has been assayed in parallel on several types of ion channels. Among interesting candidates for neuroprotection against ischemia, this work has demonstrated an interesting activating effect on neuronal K_{ATP} channels.

2. Materials and methods

2.1. Cell culture

2.1.1. Cortical embryonic mouse neurons

2.1.1.1. Primary culture of cortical neurons. Time-pregnant (E14) C57Bl6/J mice were anesthetized with isopentane followed by cervical dislocation as previously described (Heurteaux et al., 2010). Fetuses were removed and placed in cold $HBSS^+$ solution. Cerebral cortices were dissected in cold $HBSS^+$ solution and the meninges were removed. Cortical samples were cut in small pieces and were gently triturated with a fire-polished glass Pasteur pipette in 8 mL $HBSS^+$ solution. The mix was filtered (40 μm filter) and centrifuged at 800 rpm for 8 min. The supernatant was removed and the pellet was dissolved in 2 mL culture medium. Cells were plated on poly-D-lysine (Sigma–Aldrich Chimie, St Quentin Fallavier, France)-coated 12 well (24 mm diameter) plates with glass coverslips (12 mm diameter) (CML, Nemours, France) at a density of 1×10^6 cells/well in Neurobasal supplemented with B27, Glutamax, 100 units/mL penicillin, and 100 μg/mL streptomycin. Cultures were maintained at 37 °C in a humidified incubator containing 5% CO_2 and 95% air. Glial growth was suppressed by addition of 5-Fluoro-2-deoxyuridine (2 μM) and Uridine (2 μM) during the second day of culture. Cultures were used for experiments between 10 and 14 d *in vitro*.

2.1.1.2. Cos-7 cell culture. Cos-7 cells were maintained in Dulbecco's modified Eagle's medium supplemented with 10% (v/v) heat inactivated fetal bovine serum, 100 units/mL penicillin, and 100 μg/mL streptomycin and Glutamax in an atmosphere of 95% air/5% CO_2. K_{2P} channels human cDNA (25 ng hTREK-1, hTREK-2, hTRAAK, hTRESK and hTASK-1) were subcloned into the pIRES-2-eGFP vector. Cells were transfected by the JetPEI method as indicated in the manufacturer protocol (Polyplus Transfection, Poligny, France).

2.1.1.3. INS-R9 cell culture. INS-R9 cells were maintained in RPMI medium (Coppola et al., 2008) supplemented with 5% fetal calf serum, 1 mM sodium pyruvate, 2 mM glutamate, 50 mM 2-mercaptoethanol, 100 units/mL penicillin, and 100 μg/mL streptomycin in an atmosphere of 5% CO_2/95% air.

2.1.2. Oxygen glucose deprivation (OGD) model

OGD experiments were performed on primary mouse cortical neurons seeded at a density of 1,000,000 cells/35-mm dish after 12 days of culture (Goldberg and Choi, 1993). The culture medium was replaced by thorough exchange with deoxygenated glucose-free Earl's balanced salt solution (BSS). The composition of BSS solution was (in mM): 140 NaCl, 5.4 KCl, 1.2 $CaCl_2$, 0.9 $MgCl_2$, 0.44 KH_2PO_4, 4.17 $NaHCO_3$ and 0.34 Na_2HPO_4. Prior to use, BSS was equilibrated with the anaerobic gas mixture (5% CO_2, 1.2% O_2 and 93.8% N_2) by bubbling for 15 min, adjusted to pH 7.4 if necessary, and heated to 37 °C. Oxygen content of BSS was monitored with two oxygen-sensitive Clark electrodes and the Labchart 7.02 software (Powerlab, Oxford, UK). Then, cells were transferred to a humidified incubator containing a gas mixture of 5% CO_2, 1.2% O_2 and 93.8% N_2 at 37 °C. Cortical cells were subjected to 120 min OGD and allowed to recover for 24 h. OGD was terminated by removing cells from the anoxia incubator, replenishing with oxygenated Neurobasal-A medium, and replacing them in the normoxic incubator for 24 h. In these experiments cortical neurons were treated with saline, MLC901, pinacidil or glibenclamide (1 μg/mL). Treatments were applied for 2 h before OGD (pre-OGD condition), during OGD (OGD condition) or for 2 h at the end of OGD (post-OGD condition). Each condition had its own control without OGD challenge. The flowchart illustrating the experimental design is given in Fig. 1.

2.1.3. Assay of OGD-induced cell injury with Hoechst staining

Twenty hours after the OGD challenge the neuronal damage was assessed by Hoechst staining Cells were washed with phosphate buffered saline solution (PBS, Invitrogen, Saint-Aubin, France) and incubated with 2 μg/mL Hoechst (Sigma–Aldrich, Saint-Quentin Fallavier, France) for 10 min and then washed with PBS. Cells were post-fixed with 4% paraformaldehyde (PFA) at 4 °C and washed three times with PBS. Nuclei of living cells were observed by using a videomicroscope with Metafluor software. Cell counting was made automatically by Image J software. Neurons were counted for each condition, and the number of healthy neurons was calculated as the percentage of respective control for each condition. Results are expressed as mean and standard error of the mean (SEM).

2.1.4. Cell calcium imaging

Intracellular calcium concentration $[Ca^{2+}]_i$ was determined by monitoring the fluorescence intensity of a calcium indicator Fura-2 AM under an inverted fluorescent microscope (Leybaert et al., 1993). In brief, cell calcium imaging was performed on cortical neurons seeded at a density of 1,000,000 cells/35-mm fluorodish and 2 h after the 120 min-OGD challenge. Cells were treated with MLC901 (1 μg/mL) for 2 h immediately after OGD. MLC901 treatment started at the end of OGD and was applied to neurons during 120 min. A control saline-treated group was performed in the same conditions. After OGD and MLC901 treatment, cells were loaded 15–30 min with fluorescent probe Fura2-AM (10 μM) (Molecular probe, Invitrogen, Saint-Aubin, France) at 37 °C in an atmosphere of 95% air/5% CO_2. Following 30 min for dye cleavage, media was replaced by calcium imaging media contain (in mM) 116 NaCl, 5.6 KCl, 1.2 $MgCl_2$, 2 $CaCl_2$, 20 HEPES, 5 $NaHCO_3$, 1 NaH_2PO_4. Then, fluorodishes were mounted on an inverted fluorescent microscope (Zeiss, France). Cells were imaged using a plan fluor 20×0.75 oil/water immersion fluorescent objective at room temperature. Fura-2 probe was excited with alternating wavelengths 340/380 nm and images were acquired at 2 s intervals. Intracellular calcium levels were recorded using a fluorimeter-based ratiometric system. The ratio of fluorescence at 340/380 nm provides an index of intracellular Ca^{2+} concentration. In each group, at least 400 neurons were recorded from 5 independent assays. $[Ca^{2+}]_i$ was represented by the relative fluorescence intensity, $\delta F/F_0 = (F-F_0)/F_0$, where F is the fluorescence intensity measured after drug application, and F_0 is the baseline.

2.1.5. Electrophysiology

2.1.5.1. Whole cell current recordings. All electrophysiological experiments were done on INS-R9 and COS-7 transfected cells seeded at a density of 20,000 cells/35-mm dish and on cortical embryonic neurons seeded at a density of 1,000,000 cells/35-mm dish after 2–8 days of culture. COS-7 cells were transfected with 25 ng of hTREK-1, hTREK-2, hTRAAK, hTRESK, pIRES-2-eGFP vector, 25 ng of hTASK-1 pIRES-eGFP vector and hNav 1.1, hNav 1.2 pIRES-2eGFP vector. Transfected cells were used 48–72 h after transfection. All electrophysiological recordings were performed in whole cell configuration of the patch clamp technique (Hamill et al., 1981). Each current was evaluated by using a RK 400 patch clamp amplifier (Axon Instrument, USA), low-pass filtered at 3 kHz and digitized at 10 kHz using a 12-bit analog-to-digital converter digidata (1322 series, Axon Instrument, USA). All current amplitudes are expressed in current densities. Results are expressed as mean and standard error of the mean (SEM). Patch clamp pipettes were pulled using vertical puller (PC-10, Narishige) from borosilicate glass capillaries and had a resistance of 3–5 MΩ. For K^+ currents the bath solution contained (in mM) 150 NaCl, 5 KCl, 3 $MgCl_2$, 1 $CaCl_2$ and 10 HEPES adjusted to pH 7.4 with NaOH. The pipette solution contained (in mM) 155 KCl, 3 $MgCl_2$, 5 EGTA and 10 HEPES adjusted to pH 7.2 with KOH. For Na^+ currents, the bath solution contained (in mM) 150 NaCl, 2 KCl, 1 $MgCl_2$, 1.5 $CaCl_2$, 10 glucose and 10 HEPES adjusted to pH 7.4 with NaOH. The pipette solution contained (in mM) 135 CsCl, 2 $MgCl_2$, 2.5 Na_2-ATP, 5 EGTA, 2.1 $CaCl_2$, and 10 HEPES adjusted to pH 7.2 with CsOH. All experiments were performed at room temperature (21–22°C). Stimulation protocols and data acquisition were carried out using a microcomputer (Dell Pentium) witch used a commercial software and hardware (pClamp 8.2). K^+ currents were recorded by voltage clamp steps to membrane potentials of −140 to +80 mV for neurons or −100 to +60 mV for transfected cell lines in 20 mV steps applied from a holding potential of −80 mV. Duration of depolarization pulses were 0.825 ms, and the pulse cycling rate was 5 s. Current amplitudes were evaluated at the end of the stimulation pulses. Na^+ currents were recorded by voltage clamp steps to membrane potentials of −80 to +50 mV in 5 mV steps applied from a holding potential of −100 mV. The duration of a depolarization pulse was 100 ms, and the pulse cycling rate was 2 s. Current amplitudes were evaluated at the peak of the stimulation pulses. To isolate the native Na^+ currents, tetraethylammonium (TEA) was used in the extracellular solution to block K^+ channels. The presence of cadmium in the extracellular solution allowed the blockade of calcium currents in these neurons. Cells were continuously superfused with a microperfusion system. For COS-7 transfected cells, TREK-1, TREK-2 and TRAAK currents were evaluated in the presence of a cocktail of potassium channel inhibitors (K^+ blockers: 3 mM 4-aminopyridine (4-AP), 10 mM TEA, 10 μM glibenclamide, 100 nM apamin and 50 nM charybdotoxin) constituting the control conditions. MLC901 (1 μg/mL) was added to these control conditions, and validation of current activation was obtained using a pharmacological activator arachidonic acid (10 μM) of TREK-1, TREK-2 and TRAAK currents. TASK-1, TRESK-1, Nav 1.1 and Nav1.2 currents were evaluated in the control conditions and in the presence of MLC901 (1 μg/mL). For INS-R9 cells, currents were recorded in control conditions, then in the presence of MLC901 (1 μg/mL), MLC901 + Pinacidil (10 μM) and MLC901 + Pinacidil + Glibenclamide (10 μM). Control, Pinacil, Pinacidil + MLC901 and

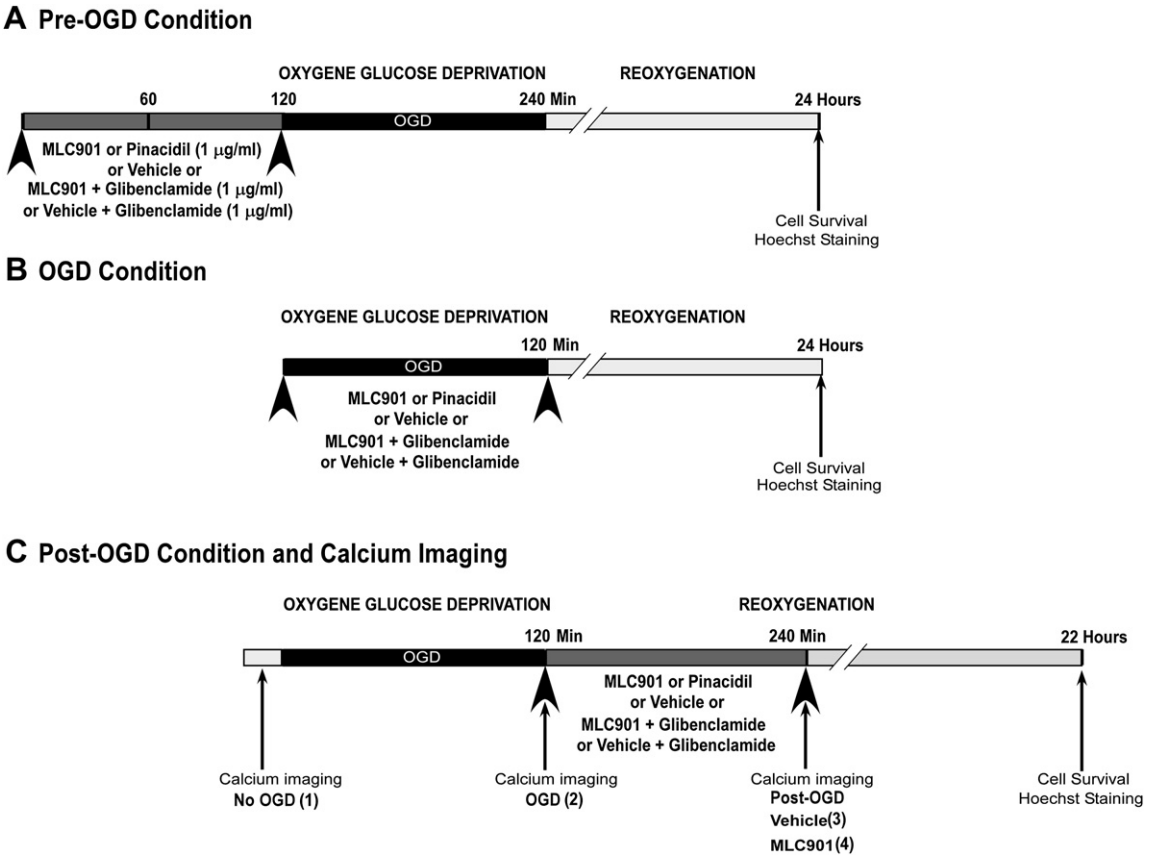

Fig. 1. Flowchart illustrating the different *in vitro* protocols. In A, B and C, cells were subjected to a 120 min oxygen glucose deprivation. (A): *Pre-OGD condition*, MLC901, Pinacidil (1 μg/mL), Vehicle or MLC901 + Glibenclamide (1 μg/mL) was applied to the cells during 2 h before OGD, (B) *OGD condition*, MLC901, Pinacidil (1 μg/mL), Vehicle or MLC901+ Glibenclamide (1 μg/mL) was applied to the cells during the 120 min of OGD, (C) *Post-OGD condition*, MLC01, Pinacidil (1 μg/mL), Vehicle or MLC901 + Glibenclamide (1 μg/mL) was applied to the cells at the end of OGD during 2 h. Cells allowed to recover for 24 h in normoxic conditions and cell death was assessed by Hoechst staining. For calcium imaging, there were 4 groups: 1/without OGD, 2/at the end of OGD, 3/OGD + Vehicle and 4/OGD+MLC901 (1 μg/mL). Measures of $[Ca^{2+}]_i$ in groups 3 and 4 were performed 2 h after the end of OGD.

Pinacidil + MLC901 + Glibenclamide (10 μM) sequence perfusion was also performed. On cortical neurons, K^+ currents were recorded in control conditions, in the presence of MLC901 and in the presence of MLC901 before and after Glibenclamide (10 μM) perfusion. MLC901 was also tested on global currents after Pinacidil (10 μM) perfusion. Na^+ currents were recorded on cortical neurons in control conditions and in the presence of MLC901 (1 μg/mL).

2.1.5.2. Oocyte recordings. Defolliculated Xenopus oocytes were injected with 100 nL of cRNA at 0.02–0.4 μg/μL for Kir 6.2 and SUR 2A expression, and recorded 2–4 days later. For electrophysiology, single oocytes were placed in a 0.3-mL perfusion chamber and impaled with two standard microelectrodes (1–2.5 MΩ resistance) filled with 3 M KCl and voltage clamped with a Dagan CA-1 amplifier, in symmetrical potassium solution containing (in mM) (90 KCl, 1.8 $CaCl_2$, 1 mM $MgCl_2$, 5 Hepes, pH 7.4 with KOH). Stimulation of the preparation, data acquisition, and analysis were performed using pClamp software (Axon Instruments). Currents were recorded in this potassium symmetrical control condition. K_{ATP} channel activity was evaluated by intracellular ATP depletion by 3 mM of sodium azide. MLC901 (1 μg/mL) and Pinacidil (10 μM) were tested before and after ATP depletion in oocytes. In all experiments, inhibition by Glibenclamide (10 μM) of recorded currents was evaluated.

2.1.5.3. Membrane potential measurements. Membrane potentials were measured on cortical neurons. Cells were incubated during 24 h in control conditions, in the presence of MLC901 (1 μg/mL), MLC901 + Glibenclamide (10 μM), MLC901 + Pinacidil (10 μM), and MLC901 + Pinacidil (1 μg/mL) + Glibenclamide (10 μM). After the incubation period, cells were patched and membrane potentials were immediately measured using the whole cell patch clamp configuration. All values of membrane potentials are expressed in mV as mean ± standard error of the mean (SEM).

2.1.5.4. Statistical analyses. Data were expressed as mean ± S.E.M. Statistical analysis of differences between groups was performed by using unpaired *t* test or ANOVA. In all analyses, the level of significance was set at $^*P < 0.05$, $^{**}P < 0.01$, $^{***}P < 0.001$.

3. Results

3.1. MLC901 protects cortical neurons against death and exaggerated calcium influx associated with oxygen glucose deprivation

The effects of MLC901 were studied in an *in vitro* model of ischemia in which 12 day old primary cortical neurons were exposed to 120 min oxygen and glucose deprivation. Hoechst staining of nuclei of living neurons was used to assess OGD-induced neuronal death in neurons. Cortical neurons were first treated with saline or MLC901 (1 μg/mL). The dose of MLC901 used was selected based on our previous study, where the application of 1 μg/mL MLC901-induced the best protection against cell death on cortical neurons in culture (Heurteaux et al., 2010). Cells were exposed to three treatment conditions: MLC901 was applied 1/for 2 h before OGD (pre-OGD condition), 2/during 120 min-OGD (OGD condition) and 3/for 2 h immediately after OGD (post-OGD condition) (Fig. 1). We compared the protective effects of MLC901 against OGD-induced neurodegeneration of cortical cells. Severe OGD induced a 55% decrease in the number of living Hoechst-positive cells (Fig. 2). MLC901 treatment before, during or after OGD resulted in a significant increase in neuronal viability as compared to respective controls ($n = 12$ dishes per group) (Fig. 2A–B). MLC901 application after OGD gave the better protection (Fig. 2A–B). Pinacidil, a specific K_{ATP} channel opener induced a neuronal

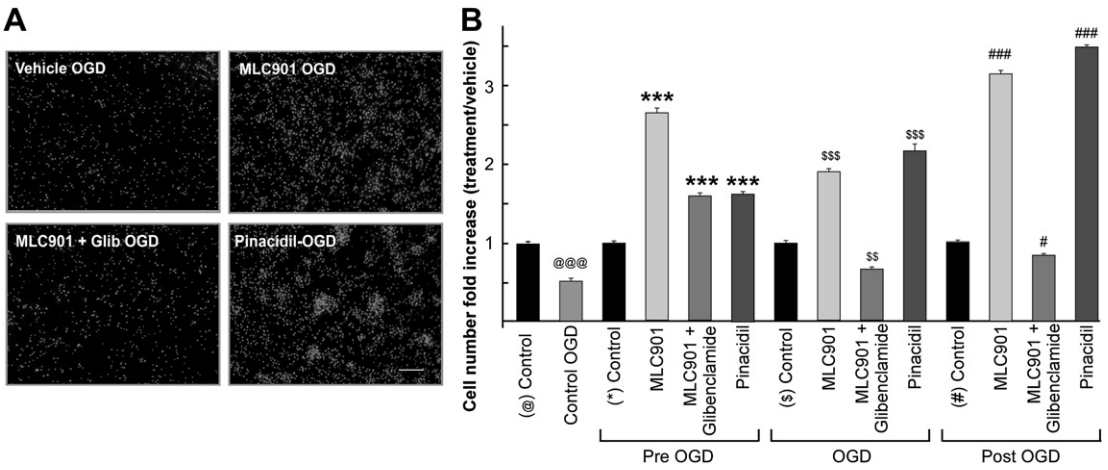

Fig. 2. Neuroprotective effect of MLC901 on neuronal death induced by oxygen glucose deprivation (OGD) and its inhibition by glibenclamide. Mature cortical neurons in culture were exposed to 120 min-OGD followed by 24 h of recovery. MLC901, Pinacidil, Vehicle or MLC901 + Glibenclamide were applied 2 h before OGD (pre-OGD), during OGD (OGD) or 2 h after OGD (post-OGD). (A) Representative photographs illustrating the protective effect of a MLC901 post-treatment on OGD-induced neuronal death and the inhibition by Glibenclamide. Prominent Hoechst staining of nuclei marked the population of living cortical neurons. (B) Histograms showing the cell number fold increase normalized by reference to respective vehicle control (Control) after MLC901, Pinacidil or Glibenclamide treatments ($n = 12$ dishes per experimental group). Scale bar = 50 μm.

protection comparable to that obtained with MLC901. An application of a specific inhibitor of K_{ATP} channels, glibenclamide (10 μM) alone (Bernardi et al., 1988; Fosset et al., 1988) or 30 min before MLC901 inhibited the protection induced by MLC901, suggesting an involvement of K_{ATP} channels in the protective effect of MLC901 against OGD damage (Fig. 2).

Dysregulation of intracellular calcium homeostasis greatly contributes to the death of neurons following an ischemic insult such as OGD. Since glutamate receptor-mediated excitotoxicity plays an important role in the process of intracellular Ca^{2+} overload (Choi, 1988), we explored whether MLC901 affected $[Ca^{2+}]_i$ induced by OGD. Experiments were conducted on cortical neurons under OGD and the effect of MLC901 on the changes in intracellular calcium fluctuations were analyzed 2 h after the end of OGD. The level of calcium fluorescence ratio obtained in the absence of OGD corresponded to the basal level of $[Ca^{2+}]_i$. Fig. 3 shows the effect of OGD alone on the changes in intracellular Ca^{2+} and the effect of MLC901 treatment applied for 2 h after the end of OGD. OGD triggered a rapid 1.55-fold increase of intracellular Fluo-4 fluorescence intensity. This was followed by a further rise in $[Ca^{2+}]_i$ during reoxygenation 2 h after OGD. Interestingly a large decrease (44.6%) in OGD-induced fluorescence intensity corresponding to intracellular Ca^{2+} was observed when MLC901 was applied during 2 h after OGD ($^{***}P < 0.001$). All these results indicate that MLC901 attenuates OGD-triggered Ca^{2+} influx and in the way contributes to protection against excitotoxicity.

3.2. The neuroprotective effect of MLC901 may be linked to K_{ATP} channel opening

K^+ channel opening leads to neuronal hyperpolarization and to a resultant decrease in cell excitability and Ca^{2+} influx. To test the hypothesis that MLC901 could in part exert its neuroprotective effect *via* a hyperpolarization, we measured its effects on the membrane potential of cortical neurons and compared it with the effect of pinacidil (Fig. 4A). An acute exposure with MLC901 or pinacidil had no effect on membrane potential (data not shown). In contrast a 24 h exposure of MLC901 or pinacidil induced a significant hyperpolarization of the membrane. The mean resting membrane potential recorded from single untreated cortical cells was −42.07 ± 2.50 mV. After 24 h of incubation with 1 μg/mL MLC901, the membrane was drastically hyperpolarized to −58.67 ± 2.92 mV. In the same conditions pinacidil induced a slight larger hyperpolarization of the membrane. Glibenclamide eliminated a large part of the hyperpolarizing action of MLC901 (Em = −46.89 ± 2.35 mV) or pinacidil (Em = 44.71 ± 3.54) (Fig. 4A). These data suggest that MLC901-induced hyperpolarization is due to an increased permeability due to activation of K_{ATP} channels.

To investigate more in details the mechanism of MLC901-induced hyperpolarization, whole-cell voltage-clamp experiments were performed on cortical neurons. Current-voltage relationships were determined before and during the application of 1 μg/mL MLC901 by applying voltage steps (20 mV increment from −150 mV to +60 mV for 0.825 ms duration) every 5 s with the membrane holding potential kept at −80 mV (Fig. 4B–D). The inversion potential in the presence or the absence of 1 μg/mL MLC901 is around to −80 mV, a value very close to K^+ equilibrium potential. MLC901 caused a clear increase in the inward currents for hyperpolarizing potentials (−140 mV to −80 mV) and also a current increase, but to a lesser extent, currents for depolarizing potentials (−70 mV to +80 mV) (Fig. 4B). Glibenclamide inhibited the MLC901-induced current (Fig. 4C). When glibenclamide was applied before MLC901, current increases were totally abolished (Fig. 4D). These results suggest that K_{ATP} channels indeed are the mediators of the MLC901-induced hyperpolarization.

To confirm these conclusions, we then carried out experiments on rat INS-R9 insulinoma cells that are known to express glibenclamide-sensitive K_{ATP} channels that are essential for insulin secretion (Amoroso et al., 1990). K_{ATP} channels in INS-R9 cells were significantly activated by MLC901 (1 μg/mL) and we observed an additive effect with the application of 10 μM pinacidil MLC901 (Fig. 5A). Interestingly, glibenclamide (10 μM) inhibited the K_{ATP} current activated by MLC901 + Pinacidil (Fig. 5A–B). Current–voltage relationships obtained in the different conditions showed that MLC901 and pinacidil behave very similarly and both are inhibited by glibenclamide (Fig. 5B). The results obtained in INS-R9 cells confirm that the effects of MLC901 are, at least in part, mediated by K_{ATP} channels.

The two subunits that constitute the neuronal K_{ATP} channel are SUR_1 and $Kir_{6.2}$ (Inagaki et al., 1995). Xenopus oocyte expression of SUR_1 and $Kir_{6.2}$ led to generation of large inwardly rectifying currents in response to application of sodium azide (3 mM) to decrease intracellular ATP (Ashcroft and Ashcroft, 1990) (Fig. 6A). The amplitude of azide-induced, glibenclamide-sensitive K_{ATP} channel current

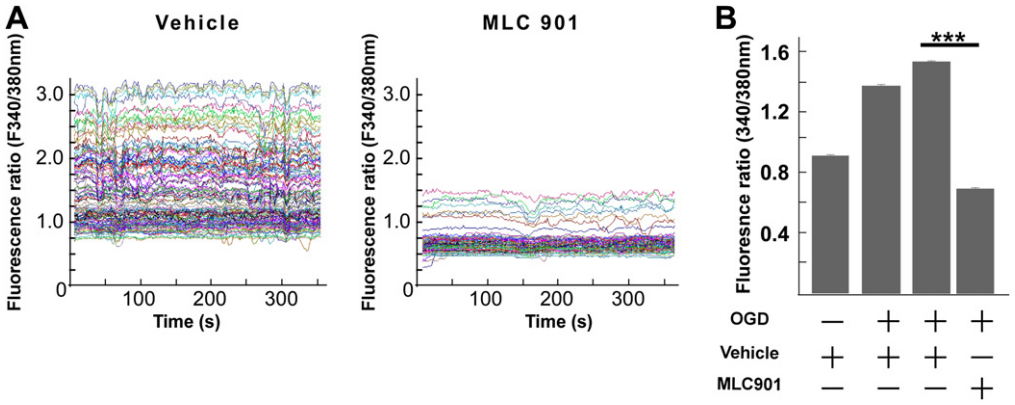

Fig. 3. Neuroprotective effect of MLC901 on calcium signaling in cortical neurons exposed to oxygen glucose deprivation (OGD). Mature cortical neurons in culture were subjected to OGD during 120 min. MLC901 (1 μg/mL) was applied 2 h after OGD. (A) Representative $[Ca^{2+}]_i$ waves imaging showing decrease of OGD-induced $[Ca^{2+}]_i$ elevation by MLC901 application (1 μg/mL) 2 h after OGD. (B) Corresponding fluorescence ratio (peak amplitude of Ca^{2+} increase by OGD in all tested conditions ($n = 5$ per condition; $^{***}P < 0.001$ *versus* vehicle group). Data are expressed as means ± SEM).

was amplified by application of pinacidil (10 μM) and, as expected, inhibited by glibenclamide (10 μM) (Fig. 6A). We then performed the same type of experiments by using MLC901. Clearly, MLC901, like pinacidil activated K_{ATP} channels revealed by the azide treatment (Fig. 6B–D). Twelve minutes after azide application, the mean current amplitude at −120 mV was −480 ± 57 nA before and −770 ± 67 after application of MLC901. This MLC901-induced activation and that produced by pinacidil, disappeared in the presence of glibenclamide (Fig. 6B–D). MLC901 behaved similarly to pinacidil by activating the K_{ATP} channel.

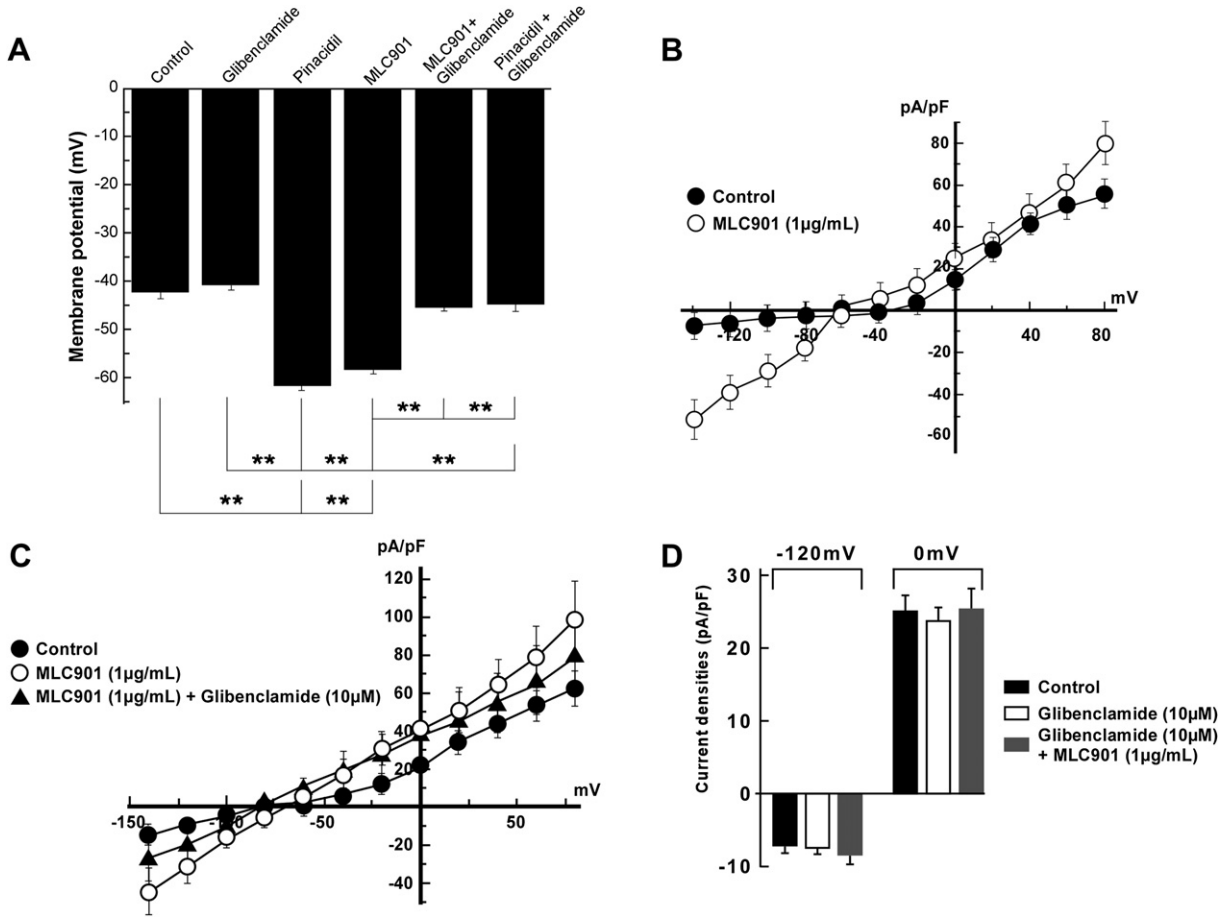

Fig. 4. Effect of MLC901 on membrane potential and current density measurements in cortical neurons. (A) Membrane potential recording after cell incubation in control conditions ($n = 25$) and in the presence of MLC901 (1 μg/mL) alone ($n = 20$; $^{***}P < 0.001$ *versus* Control group), MLC901 (1 μg/mL) + Glibenclamide (10 μM) ($n = 18$, $^{\#\#\#}P < 0.001$ *versus* MLC901 group). (B) Whole cell current–voltage relationships obtained with voltage ramps ranging from −140 to +60 mV in control conditions and in the presence of MLC901 ($n = 9$). (C) Current–voltage relationships obtained in control conditions and in the presence of MLC901 alone ($n = 22$) or MLC901 + Glibenclamide ($n = 22$). (D) Histograms showing current densities obtained in control conditions and in the presence of Glibenclamide alone ($n = 22$) or Glibenclamide + MLC901 ($n = 22$) at −120 mV and 0 mV.

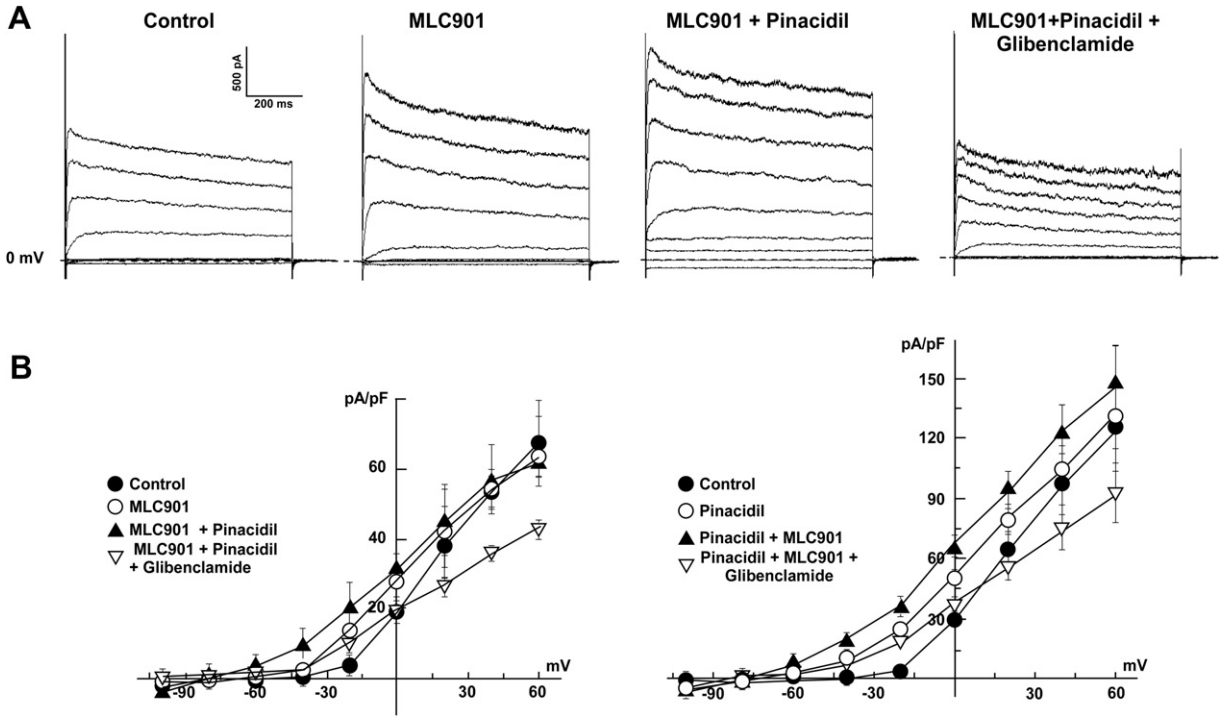

Fig. 5. Effect of MLC901 on endogenous K_{ATP} currents in INS-R9 cells. (A) Current traces recorded in control conditions and in the presence of MLC901 (1 μg/mL) alone, MLC901 (1 μg/mL) + Pinacidil (10 μM) or MLC901 (1 μg/mL) + Pinacidil (10 μM) + Glibenclamide (10 μM). (B) Left panel: Whole cell current–voltage relationships obtained with voltage ramps ranging from −100 to + 60 mV in control conditions and in the presence of MLC901 (1 μg/mL) alone, MLC901 (1 μg/mL) + Pinacidil (10 μM) or MLC901 (1 μg/mL) + Pinacidil (10 μM) + Glibenclamide (10 μM) ($n = 9$ per condition). Right panel: Whole cell current–voltage relationships obtained with voltage ramps ranging from −100 to +60 mV in control conditions and in the presence of Pinacidil (10 μM) alone, Pinacidil (10 μM) + MLC901 (1 μg/mL) or Pinacidil (10 μM) + MLC901 (1 μg/mL) + Glibenclamide (10 μM) ($n = 9$ per condition).

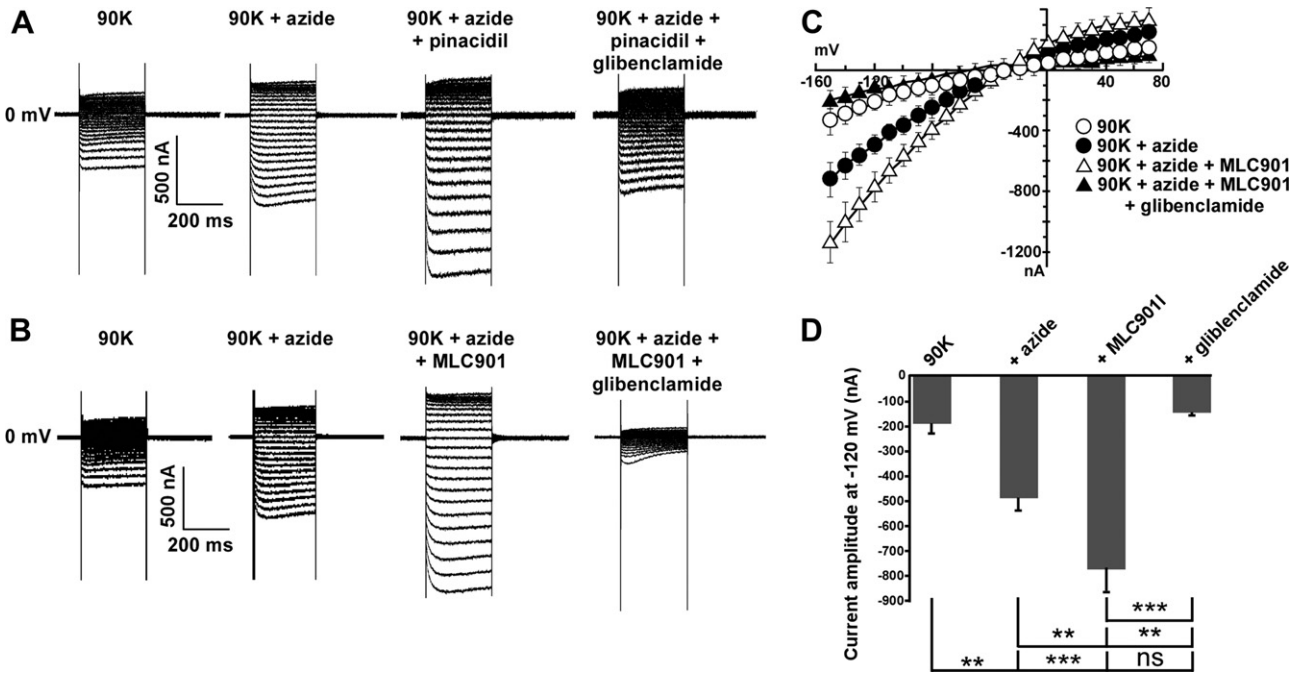

Fig. 6. Effect of MLC901 on K_{ATP} channels (Kir 6.1/SUR2) expressed in Xenopus oocytes. (A) Typical current traces recorded in control conditions (90 K, $n = 6$), in the presence of Azide (3 mM) alone or Azide + Pinacidil (10 μM) or Azide + Pinacidil + Glibenclamide (10 μM) ($n = 6$ per condition). (B) Typical current traces recorded in control conditions (90 K, $n = 6$), and in the presence of Azide (3 mM) alone, Azide + MLC901 (1 μg/mL) or Azide + MLC901 (1 μg/mL) + Glibenclamide (10 μM) ($n = 6$ per condition). (C) Whole-cell current–voltage relationships obtained with voltage ramps ranging from −160 to +80 mV in control conditions (90 K), and in the presence of Azide (3 mM) alone, Azide + MLC901 (1 μg/mL) or Azide + MLC901 (1 μg/mL) + Glibenclamide (10 μM) ($n = 6$ per condition). (D) Corresponding histograms showing the current amplitude at −120 mV for all tested conditions ($n = 6$; $^{**}P < 0.01$ and $^{***}P < 0.001$).

3.3. The neuroprotective effect of MLC901 are not linked to K_{2P} channel opening neither to Nav channel inhibition

There are other K^+ channels that may be important for neuroprotection as the two-pore domain K^+ channels (K_{2P}) when they are activated (Enyedi and Czirjak, 2010; Lesage, 2003; Lesage and Lazdunski, 2000) MLC901 was also assayed on a variety of K_{2P} channels (TREK-1, TREK-2, TRAAK, TASK and TRESK), also known to be involved in brain protection (Blondeau et al., 2007; Heurteaux et al., 2004; Lafreniere et al., 2010; Lauritzen et al., 2003). The effects of MLC901 were first analyzed on TREK-1, TREK-2 and TRAAK channels that are known to be activated by polyunsaturated fatty acids (PUFAs) and because activation of TREK-1 by PUFAs was previously found to be neuroprotective (Blondeau et al., 2009, 2002; Heurteaux et al., 2004, 2006; Lauritzen et al., 2000). Human TREK-1, TREK-2 and TRAAK cDNAs were transfected in COS-7 cells. Fig. 7A–C shows that unlike arachidonic acid, a prototype PUFA, none of these three TREK/TRAAK channels was activated by MLC901 (1 μg/mL). MLC901 was also without effect on other types of K_{2P} channels such as TASK-1 and TRESK-1 (Fig. 7D–E).

Because voltage-sensitive Na^+ channel inhibition has been correlated with neuronal protection (Gribkoff and Winquist, 2005; Obrenovitch, 1997) we also investigated the effect of MLC901 (1 μg/mL) on this channel type. Voltage-clamp recordings using the whole-cell configuration of the patch-clamp technique were first performed on cortical neurons in culture. The transient Na^+ current was evoked by step depolarization from −80 to +50 mV. Under these conditions, transient sodium currents started to activate at −60 mV and reached their maximum at −40 mV (Fig. 7F). MLC901 was without effect on these native Na^+ currents (Fig. 7F). We also examined the effect of MLC901 specifically on the Na^+ channels subtypes Nav 1.1 or the Nav 1.2 (Cantrell and Catterall, 2001; Catterall, 2000), two major subtypes of the brain voltage-gated Na^+ channels. Current–voltage relationships obtained from transfected COS-7 cells indicate that MLC901 is without effect on Nav1.1 or Nav1.2 currents (Fig. 7G–H). Voltage-gated Na^+ channels did not seem to be involved in the neuroprotective effect of MLC901.

4. Discussion

Stroke triggers a vicious cycle of electrical and chemical events, including ischemic depolarization, release of glutamate, and changes in calcium homeostasis (Dirnagl et al., 1999; Lee et al., 2000). Many of the current neuroprotective strategies have concentrated on developing drug candidates which could interfere with one or more of these processes. There are three levels of pharmaceutical intervention strategies for the treatment of stroke

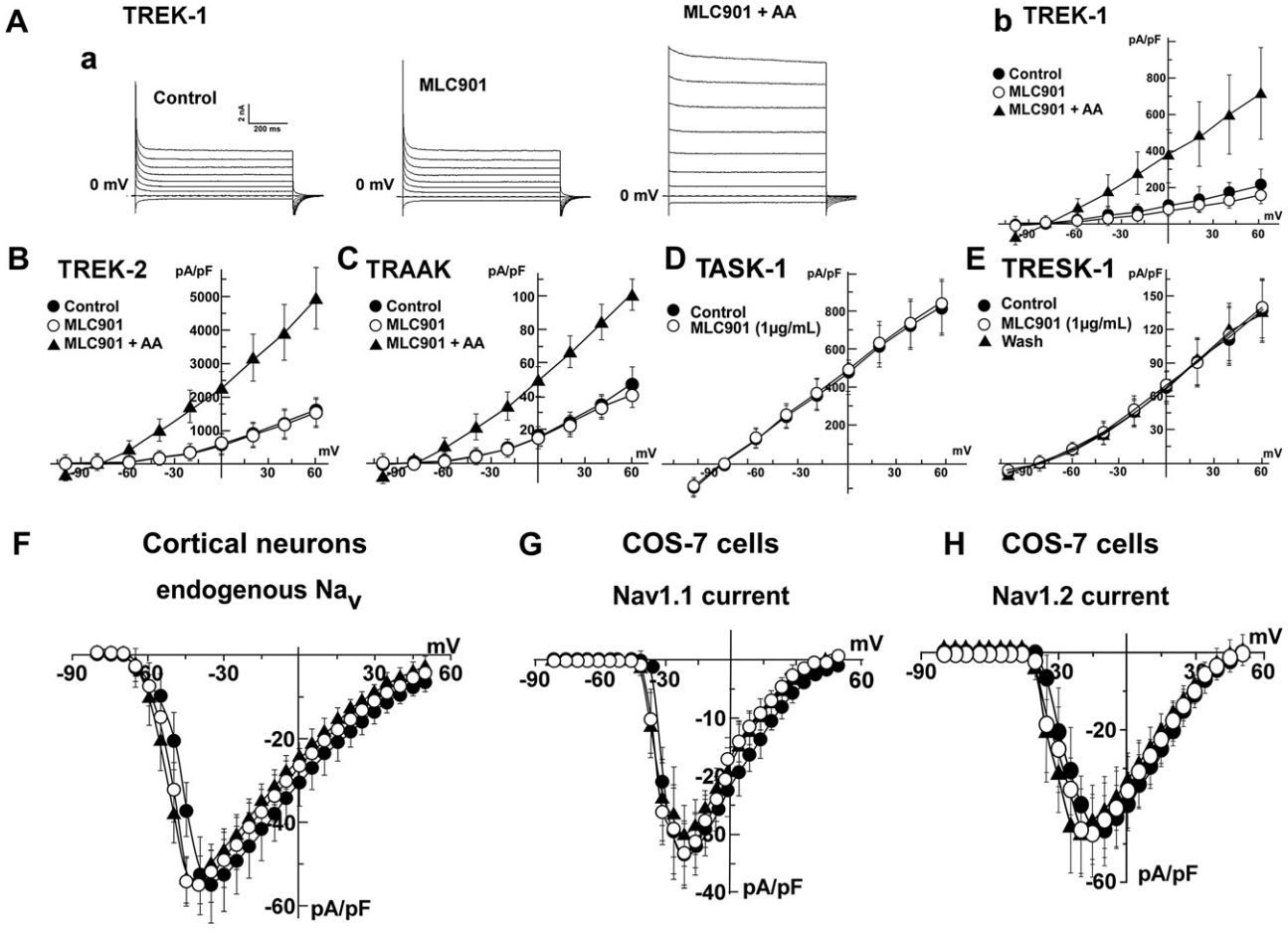

Fig. 7. Effect of MLC901 on human TREK-1, TREK-2, TRAAK, TASK-1, TRESK-1 channels and sodium channels. (A) Typical traces of TREK-1 currents (a) and corresponding whole-cell current–voltage relationships (b) obtained with voltage ramps ranging from −100 to +60 mV and recorded in control conditions and in the presence of MLC901 (1 μg/mL) alone or MLC901 (1 μg/mL) + Arachidonic acid (AA, 10 μM) ($n = 10$ per condition and for each channel). (B, C, D, E) Whole-cell current–voltage relationships of TREK-2, TRAAK, TASK-1 and TRESK-1 channels. (F) Effect of MLC901 on native sodium channels in cortical neurons in culture. Current-voltage relationships obtained in whole-cell configuration with voltage ramps ranging from −80 to +50 mV and recorded in control conditions and in the presence of MLC901 (1 μg/mL) ($n = 14$ per condition). (G–H) Effect of MLC901 on Nav1.1 (G) and Nav1.2 (H) sodium channels expressed in COS-7 cells: Current-voltage relationships obtained in whole-cell configuration with voltage ramps ranging from −80 to +50 mV and recorded in control conditions and in the presence of MLC901 (1 μg/mL) ($n = 14$ per condition).

i) preventive (prophylactic or pretreatment: anticoagulant and antiplatelet), ii) neuroprotective (early acute post-stroke treatment: thrombolytic and neuroprotective drugs), and iii) regenerative (delayed post-stroke treatment for long-term benefit: brain regeneration drugs) (Legos and Barone, 2003). Present therapeutic interventions are limited to the prophylactic level and to thrombolysis which unfortunately concerns a very small proportions of patients (Mazighi and Amarenco, 2011). Despite demonstrated efficacy in preclinical studies, most candidate neuroprotective compounds have failed in clinical trials (Lee et al., 2000). This is why we have decided to focus on alternative strategies that involve Traditional Chinese Medicine that is already used in patients in Asia, but which needs Western-type clinical trials with a solid scientific basis to support a mechanism of action. Clinical trials are on their way for NeuroAid (MLC601) (Chen et al., 2009; Venketasubramanian et al., 2009). Both MLC601 and MLC901 have emerged from recent studies *in vitro* and in rodent models as interesting candidates for stroke treatment. MLC601/MLC901 prevents glutamate excitotoxicity, necrosis and apoptosis as well as oxidative stress (Heurteaux et al., 2010). It activates the Akt survival pathway (Quintard et al., 2011). It facilitates the brain regenerative capacity following cellular/tissue loss after stroke. MLC601/MLC901 stimulates BDNF expression, enhances neurogenesis and synaptogenesis, promotes cell proliferation and stimulates neurite outgrowth (Heurteaux et al., 2010; Quintard et al., 2011).

The work described in this paper demonstrates the efficacy of MLC901 in a model of oxygen glucose deprivation, which mimics cell death processes observed in the salvageable (penumbral) regions of the ischemic brain *in vivo*. Deprivation of oxygen and glucose for 2 h on cortical neurons induced immediate neuronal swelling, followed by calcium influx observed immediately after OGD and during the early phase of reoxygenation. A subsequent neuronal degeneration occurred over the next 24 h, accompanied by release of lactate dehydrogenase (LDH) into the bathing media. MLC901 was shown to decrease OGD-triggered Ca^{2+} influx and to subsequently attenuate excitotoxicity. One cannot completely exclude an effect of MLC901 on reoxygenation but this effect, if it exists, does not seem to be important, since $[Ca^{2+}]_i$ after MLC901 treatment returned to basal levels observed before OGD and not to those after reoxygenation.

This laboratory has shown that activating K^+ channels can afford potent neuroprotection and is in fact involved in a critical way in the neuroprotective effects of preconditioning against stroke (Heurteaux et al., 1995; Plamondon et al., 1999). K^+ channel openers have potent neuroprotective properties against the deleterious effects of ischemia (Blondeau et al., 2000; Heurteaux et al., 1993, 1995; Lauritzen et al., 1997; Liss and Roeper, 2001). Because MLC901-induced hyperpolarization in cortical neurons associated with K^+ channel activation that was largely inhibited by glibenclamide, a specific blocker of K_{ATP} channels (Bernardi et al., 1988; Fosset et al., 1988) we suspected an action of this TCM on this particular class of K^+ channels. This view was confirmed when we observed the same effect of MLC901 on K_{ATP} channels of insulinoma cells in which this channel type is essential to couple changes of glucose levels to insulin secretion (Ashcroft and Ashcroft, 1990). It was also confirmed by the demonstration that co-expression of SUR_1 and $Kir_{6.2}$, the two main subunits of the neuronal K_{ATP} channel (Inagaki et al., 1995), which leads to a K^+ channel expression, particularly after ATP depletion with azide, was potently activated by MLC901. This TCM behaved in this system like pinacidil, a classical K_{ATP} channel opener (Edwards and Weston, 1990; Mannhold, 2004), and the stimulating effects of both MLC901 and pinacidil were abolished by glibenclamide. Activation of K_{ATP} channels is therefore a key event in the MLC901-induced hyperpolarization. This large hyperpolarization (~20 mV) produced by MLC901 is expected to strongly protect neurons against death. An interesting aspect of MLC901 in the OGD model is that MLC901 is more efficient when it is applied on cortical neurons after the ischemic insult as compared to a MLC901 pretreatment or during OGD. K_{ATP} channels, as their name indicates, are regulated by intracellular ATP concentrations (Aguilar-Bryan and Bryan, 1999; Nichols, 2006). High ATP concentrations close these channels and, in most cells these high concentrations are reached in physiological conditions, which means that they do not contribute, or at least do not contribute much to the membrane potential when cells and, particularly neurons are in healthy situations. However ADP also regulates the activity of this class of channels (Dunne et al., 1986; Tarasov et al., 2004; Hopkins et al., 1992). The balance between ADP and ATP levels will decide the degree of K_{ATP} channel opening. In situations of high glucose/high oxygen levels evidently the ADP/ATP ratio is very small, and K_{ATP} channels are in a closed state. Conversely, in situations of low glucose/low oxygen levels, or in situations of ischemia, the ADP/ATP ratio increases and K_{ATP} channels tend to open (Krnjevic, 2008). The efficiency of pharmacological openers of K_{ATP} channels such as pinacidil also depends on the ADP level (Aguilar-Bryan and Bryan, 1999; Edwards and Weston, 1990; Mannhold, 2004). When it increases the opener activity is favored, which means that it will be more efficient in situations of anoxia or/and ischemia. The fact that MLC901, an opener of K_{ATP} channels with properties similar to pinacidil, is more efficient after OGD is probably due to this particular property. This observation fits with the *in vivo* neuroprotective effect of MLC901 treatment against focal and global ischemia where protection is observed for treatments with MLC901 up to 3 h post-ischemia (Heurteaux et al., 2010; Quintard et al., 2011).

The activating effect of MLC901 on K_{ATP} channels are observed at therapeutic concentrations used in rodent models of ischemia. Therefore in addition to its neuroregenerative properties (Heurteaux et al., 2010), the cocktail of active molecules present in this TCM seems to act *via* K_{ATP} channels for at least a part of its properties against cerebral ischemia, keeping in mind other beneficial effects such as protection against oxidative stress, activation of the Akt kinase or stimulation of the brain derived neurotrophic factor (BDNF) (Heurteaux et al., 2010; Quintard et al., 2011).

Acknowledgments

The authors are very grateful to D. Picard (Moleac Singapore) for helpful and inspiring discussions concerning the present evaluation of the clinical effects of MLC601 and for providing MLC901. We thank Dr C. Girard and Dr M. Montegazza for the gift of K_{ATP} and Na^+ channel plasmids, respectively. This work is supported by the Centre National de la Recherche Scientifique (CNRS) and the Fondation de la Recherche Médicale (FRM: Implantation Jeune Equipe).

References

Aguilar-Bryan, L., Bryan, J., 1999. Molecular biology of adenosine triphosphate-sensitive potassium channels. Endocr. Rev. 20, 101–135.

Amoroso, S., Schmid-Antomarchi, H., Fosset, M., Lazdunski, M., 1990. Glucose, sulfonylureas, and neurotransmitter release: role of ATP-sensitive K+ channels. Science 247, 852–854.

Ashcroft, S.J., Ashcroft, F.M., 1990. Properties and functions of ATP-sensitive K-channels. Cell Signal. 2, 197–214.

Bernardi, H., Fosset, M., Lazdunski, M., 1988. Characterization, purification, and affinity labeling of the brain [3H]glibenclamide-binding protein, a putative neuronal ATP-regulated K+ channel. Proc. Natl. Acad. Sci. U S A 85, 9816–9820.

Blondeau, N., Plamondon, H., Richelme, C., Heurteaux, C., Lazdunski, M., 2000. K(ATP) channel openers, adenosine agonists and epileptic preconditioning are stress signals inducing hippocampal neuroprotection. Neuroscience 100, 465–474.

Blondeau, N., Widmann, C., Lazdunski, M., Heurteaux, C., 2002. Polyunsaturated fatty acids induce ischemic and epileptic tolerance. Neuroscience 109, 231–241.

Blondeau, N., Petrault, O., Manta, S., Giordanengo, V., Gounon, P., Bordet, R., Lazdunski, M., Heurteaux, C., 2007. Polyunsaturated fatty acids are cerebral vasodilators via the TREK-1 potassium channel. Circ. Res. 101, 176–184.

Blondeau, N., Nguemeni, C., Debruyne, D.N., Piens, M., Wu, X., Pan, H., Hu, X., Gandin, C., Lipsky, R.H., Plumier, J.C., Marini, A.M., Heurteaux, C., 2009. Subchronic alpha-linolenic acid treatment enhances brain plasticity and exerts an antidepressant effect: a versatile potential therapy for stroke. Neuropsychopharmacology 34, 2548–2559.

Cantrell, A.R., Catterall, W.A., 2001. Neuromodulation of Na+ channels: an unexpected form of cellular plasticity. Nat. Rev. Neurosci. 2, 397–407.

Catterall, W.A., 2000. From ionic currents to molecular mechanisms: the structure and function of voltage-gated sodium channels. Neuron 26, 13–25.

Chen, C., Venketasubramanian, N., Gan, R.N., Lambert, C., Picard, D., Chan, B.P., Chan, E., Bousser, M.G., Xuemin, S., 2009. Danqi Piantang Jiaonang (DJ), a traditional Chinese medicine, in poststroke recovery. Stroke 40, 859–863.

Choi, D.W., 1988. Glutamate neurotoxicity and diseases of the nervous system. Neuron 1, 623–634.

Coppola, T., Beraud-Dufour, S., Antoine, A., Vincent, J.P., Mazella, J., 2008. Neurotensin protects pancreatic beta cells from apoptosis. Int. J. Biochem. Cell Biol. 40, 2296–2302.

Dirnagl, U., Iadecola, C., Moskowitz, M.A., 1999. Pathobiology of ischaemic stroke: an integrated view. Trends Neurosci. 22, 391–397.

Dunne, M.J., Findlay, I., Petersen, O.H., Wollheim, C.B., 1986. ATP-sensitive K+ channels in an insulin-secreting cell line are inhibited by D-glyceraldehyde and activated by membrane permeabilization. J. Membr. Biol. 93, 271–279.

Edwards, G., Weston, A.H., 1990. Structure-activity relationships of K+ channel openers. Trends Pharmacol. Sci. 11, 417–422.

Enyedi, P., Czirjak, G., 2010. Molecular background of leak K+ currents: two-pore domain potassium channels. Physiol. Rev. 90, 559–605.

Fosset, M., De Weille, J.R., Green, R.D., Schmid-Antomarchi, H., Lazdunski, M., 1988. Antidiabetic sulfonylureas control action potential properties in heart cells via high affinity receptors that are linked to ATP-dependent K+ channels. J. Biol. Chem. 263, 7933–7936.

Gan, R., Lambert, C., Lianting, J., Chan, E.S., Venketasubramanian, N., Chen, C., Chan, B.P., Samama, M.M., Bousser, M.G., 2008. Danqi Piantan Jiaonang does not modify hemostasis, hematology, and biochemistry in normal subjects and stroke patients. Cerebrovasc. Dis. 25, 450–456.

Goldberg, M.P., Choi, D.W., 1993. Combined oxygen and glucose deprivation in cortical cell culture: calcium-dependent and calcium-independent mechanisms of neuronal injury. J. Neurosci. 13, 3510–3524.

Gribkoff, V.K., Winquist, R.J., 2005. Voltage-gated cation channel modulators for the treatment of stroke. Expert Opin. Investig. Drugs 14, 579–592.

Hamill, O.P., Marty, A., Neher, E., Sakmann, B., Sigworth, F.J., 1981. Improved patch-clamp techniques for high-resolution current recording from cells and cell-free membrane patches. Pflugers Arch. 391, 85–100.

Heurteaux, C., Bertaina, V., Widmann, C., Lazdunski, M., 1993. K+ channel openers prevent global ischemia-induced expression of c-fos, c-jun, heat shock protein, and amyloid beta-protein precursor genes and neuronal death in rat hippocampus. Proc. Natl. Acad. Sci. U S A 90, 9431–9435.

Heurteaux, C., Lauritzen, I., Widmann, C., Lazdunski, M., 1995. Essential role of adenosine, adenosine A1 receptors, and ATP-sensitive K+ channels in cerebral ischemic preconditioning. Proc. Natl. Acad. Sci. U S A 92, 4666–4670.

Heurteaux, C., Guy, N., Laigle, C., Blondeau, N., Duprat, F., Mazzuca, M., Lang-Lazdunski, L., Widmann, C., Zanzouri, M., Romey, G., Lazdunski, M., 2004. TREK-1, a K(+) channel involved in neuroprotection and general anesthesia. Embo J. 23, 2684–2695.

Heurteaux, C., Laigle, C., Blondeau, N., Jarretou, G., Lazdunski, M., 2006. Alpha-linolenic acid and riluzole treatment confer cerebral protection and improve survival after focal brain ischemia. Neuroscience 137, 241–251.

Heurteaux, C., Gandin, C., Borsotto, M., Widmann, C., Brau, F., Lhuillier, M., Onteniente, B., Lazdunski, M., 2010. Neuroprotective and neuroproliferative activities of NeuroAid (MLC601, MLC901), a Chinese medicine, in vitro and in vivo. Neuropharmacology 58, 987–1001.

Hopkins, W.F., Fatherazi, S., Peter-Riesch, B., Corkey, B.E., Cook, D.L., 1992. Two sites for adenine-nucleotide regulation of ATP-sensitive potassium channels in mouse pancreatic beta-cells and HIT cells. J. Membr. Biol. 129, 287–295.

Inagaki, N., Gonoi, T., Clement IV, J.P., Namba, N., Inazawa, J., Gonzalez, G., Aguilar-Bryan, L., Seino, S., Bryan, J., 1995. Reconstitution of IKATP: an inward rectifier subunit plus the sulfonylurea receptor. Science 270, 1166–1170.

Krnjevic, K., 2008. Electrophysiology of cerebral ischemia. Neuropharmacology 55, 319–333.

Lafreniere, R.G., Cader, M.Z., Poulin, J.F., Andres-Enguix, I., Simoneau, M., Gupta, N., Boisvert, K., Lafreniere, F., McLaughlan, S., Dube, M.P., Marcinkiewicz, M.M., Ramagopalan, S., Ansorge, O., Brais, B., Sequeiros, J., Pereira-Monteiro, J.M., Griffiths, L.R., Tucker, S.J., Ebers, G., Rouleau, G.A., 2010. A dominant-negative mutation in the TRESK potassium channel is linked to familial migraine with aura. Nat. Med. 16, 1157–1160.

Lauritzen, I., De Weille, J.R., Lazdunski, M., 1997. The potassium channel opener (-)-cromakalim prevents glutamate-induced cell death in hippocampal neurons. J. Neurochem. 69, 1570–1579.

Lauritzen, I., Blondeau, N., Heurteaux, C., Widmann, C., Romey, G., Lazdunski, M., 2000. Polyunsaturated fatty acids are potent neuroprotectors. EMBO J. 19, 1784–1793.

Lauritzen, I., Zanzouri, M., Honore, E., Duprat, F., Ehrengruber, M.U., Lazdunski, M., Patel, A.J., 2003. K+-dependent cerebellar granule neuron apoptosis. Role of task leak K+ channels. J. Biol. Chem. 278, 32068–32076.

Lee, J.M., Grabb, M.C., Zipfel, G.J., Choi, D.W., 2000. Brain tissue responses to ischemia. J. Clin. Invest. 106, 723–731.

Legos, J.J., Barone, F.C., 2003. Update on pharmacological strategies for stroke: prevention, acute intervention and regeneration. Curr. Opin. Investig. Drugs 4, 847–858.

Lesage, F., Lazdunski, M., 2000. Molecular and functional properties of two pore domain potassium channels. Am. J. Physiol. 279, 793–801.

Lesage, F., 2003. Pharmacology of neuronal background potassium channels. Neuropharmacology 44, 1–7.

Leybaert, L., De Ley, G., de Hemptinne, A., 1993. Effects of flunarizine on induced calcium transients as measured in fura-2-loaded neurons of the rat dorsal root ganglion. Naunyn Schmiedebergs Arch. Pharmacol. 348, 269–274.

Liss, B., Roeper, J., 2001. Molecular physiology of neuronal K_{ATP} channels (review). Mol. Membr. Biol. 18, 117–127.

Mannhold, R., 2004. K_{ATP} channel openers: structure-activity relationships and therapeutic potential. Med. Res. Rev. 24, 213–266.

Mazighi, M., Amarenco, P., 2011. Reperfusion therapy in acute cerebrovascular syndrome. Curr. Opin. Neurol. 24, 59–62.

Nichols, C.G., 2006. KATP channels as molecular sensors of cellular metabolism. Nature 440, 470–476.

Obrenovitch, T.P., 1997. Sodium and potassium channel modulators: their role in neuroprotection. Int. Rev. Neurobiol. 40, 109–135.

Plamondon, H., Blondeau, N., Heurteaux, C., Lazdunski, M., 1999. Mutually protective actions of kainic acid epileptic preconditioning and sublethal global ischemia on hippocampal neuronal death: involvement of adenosine A1 receptors and K(ATP) channels. J. Cereb. Blood Flow Metab. 19, 1296–1308.

Quintard, H., Borsotto, M., Veyssiere, J., Gandin, C., Labbal, F., Widmann, C., Lazdunski, M., Heurteaux, C., 2011. MLC901, a traditional Chinese medicine protects the brain against global ischemia. Neuropharmacology 61, 622–631.

Shahripour, R.B., Shamsaei, G., Pakdaman, H., Majdinasab, N., Nejad, E.M., Sajedi, S.A., Norouzi, M., Hemmati, A., Manouchehri, R.H., Shiravi, A., 2011. The effect of NeuroAid (MLC601) on cerebral blood flow velocity in subjects' post brain infarct in the middle cerebral artery territory. Eur. J. Intern. Med. 22, 509–513.

Tarasov, A., Dusonchet, J., Ashcroft, F., 2004. Metabolic regulation of the pancreatic beta-cell ATP-sensitive K+ channel: a pas de deux. Diabetes 53 (Suppl. 3), S113–S122.

Venketasubramanian, N., Chen, C.L., Gan, R.N., Chan, B.P., Chang, H.M., Tan, S.B., Picard, D., Navarro, J.C., Baroque 2nd, A.C., Poungvarin, N., Donnan, G.A., Bousser, M.G., 2009. A double-blind, placebo-controlled, randomized, multi-center study to investigate CHInese Medicine Neuroaid Efficacy on Stroke recovery (CHIMES Study). Int. J. Stroke 4, 54–60.

Young, S.H., Zhao, Y., Koh, A., Singh, R., Chan, B.P., Chang, H.M., Venketasubramanian, N., Chen, C., 2010. Safety profile of MLC601 (Neuroaid) in acute ischemic stroke patients: a Singaporean substudy of the Chinese medicine neuroaid efficacy on stroke recovery study. Cerebrovasc. Dis. 30, 1–6.